Journal of Magnetic Resonance 201 (2009) 81–86

Contents lists available at ScienceDirect

Journal of Magnetic Resonance

journal homepage: www.elsevier.com/locate/jmr

Q-shear transformation for MQMAS and STMAS NMR spectra

Ivan Hung [a], Julien Trébosc [b], Gina L. Hoatson [c], Robert L. Vold [d], Jean-Paul Amoureux [b], Zhehong Gan [a,*]

[a] Center of Interdisciplinary Magnetic Resonance, National High Magnetic Field Laboratory, 1800 East Paul Dirac Drive, Tallahassee, FL 32310, USA
[b] Unité de Catalyse et Chimie du Solide, UMR-CNRS 8181, Université de Lille 1, 59652 Villeneuve d'Ascq cedex, France
[c] Department of Physics, College of William and Mary, P.O. Box 8795, Williamsburg, VA 23187-8795, USA
[d] Department of Applied Science, College of William and Mary, P.O. Box 8795, Williamsburg, VA 23187-8795, USA

ARTICLE INFO

Article history:
Received 7 July 2009
Revised 7 August 2009
Available online 15 August 2009

Keywords:
MQMAS
STMAS
Representation
Shearing transformation
^{45}Sc
^{93}Nb
Isotropic

ABSTRACT

The multiple-quantum magic-angle spinning (MQMAS) and satellite-transition magic-angle spinning (STMAS) experiments refocus second-order quadrupolar broadening of half-integer quadrupolar spins in the form of two-dimensional experiments. Isotropic shearing is usually applied along the indirect dimension of the 2D spectra such that an isotropic projection free of anisotropic quadrupolar broadening can be obtained. An alternative shear transformation by a factor equal to the coherence level (quantum number) selected during the evolution period is proposed. Such a transformation eliminates chemical shift along the indirect dimension leaving only the second-order quadrupolar-induced shift and anisotropic broadening, and is expected to be particularly useful for disordered systems. This transformation, dubbed *Q*-shearing, can help avoid aliasing problems due to large chemical shift ranges and spinning sidebands. It can also be used as an intermediate step to the isotropic representation for expanding the spectral window of rotor-synchronized experiments.

1. Introduction

The multiple-quantum magic-angle spinning (MQMAS) [1] and later satellite-transition magic-angle spinning (STMAS) [2] experiments have been developed to refocus the second-order quadrupolar broadening in the form of two-dimensional spectroscopy. The correlation of multiple-quantum or satellite transitions with the central transition of half-integer spins yields tilted ridge-shaped peaks in the 2D spectra. Isotropic spectra free of anisotropic broadening can be obtained by a shear transformation along the indirect dimension of the 2D spectra.

Since the introduction of these experiments, many schemes for improving the efficiency [3–9] and various methods for acquiring absorptive 2D spectra [10,11] have been developed. This contribution addresses a few remaining issues of possible concern. First, rotor synchronization of the evolution period (t_1) is a must for STMAS [12] and is strongly desired for MQMAS [13] in order to enhance peak intensities by overlaying/aliasing spinning sidebands. Rotor synchronization of t_1 limits the indirect spectral window to the spinning frequency, which is often insufficient to cover the chemical shift range especially at high magnetic fields. Peaks outside the window are aliased or folded back hindering spectral interpretation. The second issue concerns spinning sidebands associated with large chemical shift anisotropy and quadrupolar coupling. With a rotor-synchronized t_1 evolution, spinning sidebands indeed appear only along the direct dimension (F_2). However, isotropic shearing with non-integer factors shifts spinning sidebands so that they appear in the indirect dimension (F_{iso}) as well. These numerous sidebands alias back into the small F_{iso} window complicating the isotropic projection and spectral interpretation.

In this paper, an alternative shear transformation by a factor equal to the coherence level selected during the t_1 period is proposed [14], for example, 3 for triple-quantum (3Q) MAS, 1 for (1Q) STMAS and 2 for double-quantum (2Q) STMAS [15]. This transformation is dubbed *Q*-shearing because it eliminates the chemical shift, leaving only the second-order quadrupolar-induced shift and anisotropic broadening along the indirect dimension (F_Q) of the *Q*-sheared spectrum. In some aspects this method bears similarities to recent reports on shearing of multiple-quantum spectra acquired under conditions of 70.12° spinning [16] and double rotation [17]. It will be shown that chemical shift elimination can solve the aforementioned problems effectively. The *Q*-shear transformation gives a simple and unified representation for MQMAS and STMAS spectra, especially for disordered samples for which isotropic shearing does not necessarily yield high spectral resolution. In the case where isotropic spectra of crystalline samples free of aliasing are desirable, zero-filling in the frequency-domain of *Q*-sheared spectra is proposed as an intermediate step to the isotropic representation. In this way, the spectral window can be expanded at will such that spinning sidebands appear in an orderly fashion without aliasing/folding. It should be noted that *all shear*

* Corresponding author. Fax: +1 850 644 1366.
E-mail address: gan@magnet.fsu.edu (Z. Gan).

1090-7807/$ - see front matter © 2009 Elsevier Inc. All rights reserved.
doi:10.1016/j.jmr.2009.08.007

transformations are only changes of representation for the convenience of spectral interpretation; *the information content of the spectra* (*including* resolution and signal-to-noise ratio) *remains unchanged from its original representation.*

2. Isotropic shear and *Q*-shear transformations

The MQMAS [18] and STMAS [12] experiments rely on the fact that for the different transitions involved in a MAS experiment the expansion coefficients of the second-order quadrupolar interaction are related to each other by certain constant ratios k_q^l [19], where q denotes the experiment type, i.e., the t_1-evolution coherence level. These can be derived from the ratio R^l_{S,m_S} between the expansion coefficients of any single-quantum transition ($m_S + 1/2 \Longleftrightarrow m_S - 1/2$) and the central transition ($m_S = 0$),

$$R^0_{S,m_S} = 1 - \frac{36m_S^2}{4S(S+1)-3}, \quad R^4_{S,m_S} = 1 - \frac{68m_S^2}{3[4S(S+1)-3]} \tag{1}$$

where S is the spin quantum number. For example, for a 2Q satellite-transition the ratio is the sum of the central transition and one first-satellite transition ($k_2^l = R^l_{S,0} + R^l_{S,1}$), for a 3Q transition the sum of the central transition and twice the first-satellite transition ($k_3^l = R^l_{S,0} + 2R^l_{S,1}$), for 5Q transitions it is equal to the central transition plus twice the first- and second-satellite transitions ($k_5^l = R^l_{S,0} + 2R^l_{S,1} + 2R^l_{S,2}$). The ratios k_q^l and multiple-quantum numbers selected during t_1 evolution (q) are listed in Table 1 for the MQMAS and STMAS experiments. Only the $l = 0$ and 4 rank terms are listed because the $l = 2$ term is averaged to zero by MAS. The $l = 0$ term only shifts the peak position whereas the $l = 4$ term is responsible for anisotropic broadening. In two-dimensional MQMAS and STMAS spectra, the correlation between two inhomogeneously broadened transitions yields a ridge tilted at slope k_q^4 and centered at $(q \cdot \upsilon_{CS} + k_q^0 \cdot \upsilon_{QIS}, \upsilon_{CS} + \upsilon_{QIS})$ in the (F_1, F_2) coordinates. Here υ_{CS} and $\upsilon_{QIS} = 3P_Q^2[3/4 - S(S+1)]/\{10\upsilon_0[2S(2S-1)]^2\}$ are the chemical and quadrupolar-induced shifts of the central transition in *hertz* along F_2, with $P_Q = C_Q\sqrt{1+\eta_Q^2/3}$. The ratio of the chemical shift along the two frequencies F_1 and F_2 is equal to the quantum number q during t_1.

In their original representation, the MQMAS and STMAS experiments do not yield an isotropic projection along F_1 or F_2 directly. An isotropic projection can be obtained by two methods. The first and most commonly used method is by shearing 2D spectra along F_1 in the frequency-domain such that the tilted peaks become parallel to the F_2 axis [18,20]; this method is denoted herein as 'isotropic shearing'. Projection onto the new F_1 axis (henceforth called F_{iso}) becomes free of anisotropic broadening yielding an isotropic spectrum. The other, so-called "split-t_1," method [21,22] is performed in the time domain by including a part of $t_2 = |k_q^4| \cdot t_1$ into the redefined evolution period, such that the echo from refocusing of the anisotropic broadening remains stationary in t_2 while t_1 is incremented. Fourier transformation of "split-t_1" 2D data yields isotropic spectra directly. In principle, the two methods are equivalent according to the similarity theorem of Fourier spectroscopy [23]. In fact, the conventional implementation of frequency-domain shearing is performed by t_1-dependent first-order phasing in the mixed time–frequency domain (t_1, F_2) [20], which translates into a redefinition of the evolution period in the same way as the "split-t_1" method. A detailed comparison of these methods can be found in Ref. [10]. The focus of the present work is on frequency-domain transformation, the time-domain equivalence of *Q*-shearing is not discussed further here.

Mathematically, isotropic shearing replaces F_1 with F_{iso},

$$F_{iso} = (F_1 - k_q^4 F_2)/(1 + |k_q^4|) \tag{2}$$

while *Q*-shearing, which replaces F_1 with F_Q, differs only by the slope q

$$F_Q = (F_1 - qF_2)/(1 + |q|) \tag{3}$$

It should be noted that shearing can in principle be carried out on either dimension. In this instance, the F_1 dimension has been chosen for shearing so that spectra along the un-sheared F_2 dimension can be readily compared with, and used to reconstruct, 1D MAS spectra.

Table 1
Indirect dimension evolution quantum numbers (q) and ratios for the 0th- and 4th-rank second-order quadrupolar terms in various STMAS and MQMAS experiments with spin S up to 9/2.

	1Q STMAS	2Q STMAS	3QMAS	5QMAS	7QMAS	9QMAS
q	1	2	3	5	7	9
$S = 3/2$ k_q^0	−2	−1	−3	–	–	–
k_q^4	−8/9	1/9	−7/9			
$S = 5/2$	−1/8	7/8	3/4	−25/4	–	–
	7/24	31/24	19/12	−25/12		
$S = 7/2$	2/5	7/5	9/5	−1	−49/5	–
	28/45	73/45	101/45	11/9	−161/45	
$S = 9/2$	5/8	13/8	9/4	5/4	−7/2	−27/2
	55/72	127/72	91/36	95/36	7/18	−31/6

3. Labeling and scaling of the sheared F_1 axis

Shear transformations change the appearance of 2D MQMAS and STMAS spectra for easier spectral interpretation. However, for quantitative analysis of the sheared spectra (e.g., using DMFIT [24]), it is important to label the new axis and define scaling factors for the chemical and quadrupolar shifts. These seemingly trivial tasks are complicated by the shear transformation. The scaling factors employed and their rationales are presented below (all discussions in the following are with respect to the F_1 dimension, as F_2 is not altered).

In the original representations, the F_1 spectral window in *hertz* is equal to $SW_1 = 1/dw_1$ where dw_1 is the t_1 dwell time. The first consequence of isotropic shearing is scaling of the spectral window in *hertz* (Eqs. (2) and (3)), which is necessary according to the Nyquist theorem,

$$SW_{iso}(Hz) = SW_1(Hz)/(1 + |k_q^4|) \tag{4}$$

The chemical and quadrupolar-induced shift frequencies (in *hertz*) along F_{iso} become

$$\upsilon_{CS}^{F_{iso}} = [(q - k_q^4)/(1 + |k_q^4|)] \cdot \upsilon_{CS} = \kappa_{iso}^{CS} \cdot \upsilon_{CS} \tag{5}$$

$$\upsilon_{QIS}^{F_{iso}} = [(k_q^0 - k_q^4)/(1 + |k_q^4|)] \cdot \upsilon_{QIS} = \kappa_{iso}^{0} \cdot \upsilon_{QIS} \tag{6}$$

The chemical shift scale in *ppm* has been somewhat artificially defined in order to have the same chemical shift in *ppm* along both dimensions for any arbitrary spin value and t_1-evolution quantum number [25]. This is done by dividing $\upsilon_{CS}^{F_{iso}}$ with the apparent Larmor frequency $\upsilon_0 \cdot (q - k_q^4)/(1 + |k_q^4|)$. Such a scaling changes the spectral window in *ppm* to

$$\begin{aligned} SW_{iso}(ppm) &= SW_{iso}(Hz) \cdot (1 + |k_q^4|)/[(q - k_q^4) \cdot \upsilon_0] \\ &= SW_1(Hz)/[(q - k_q^4) \cdot \upsilon_0] \end{aligned} \tag{7}$$

The chemical shift reference in *ppm* remains unchanged, i.e., the carrier/transmitter frequency has the same *ppm* shift in both F_{iso}

and F_2. However, this procedure has some unintended consequences: the spacing between spinning sidebands is no longer the same in F_{iso} and F_2, and the slope of central-transition diagonal peaks in STMAS spectra is equal to 1 in *ppm* but not in units of *hertz*. This *ppm* chemical shift scale is often applied for labeling of the isotropically sheared axis, although controversy still remains regarding its application due to the calculation of *ppm* units with a scaled Larmor frequency. Further discussions on this issue can be found in references [26,27]. With this chemical shift scaling, the quadrupolar-induced shift in *ppm* is given by

$$\delta_{QIS}^{F_{iso}} = [(k_q^0 - k_q^4)/(q - k_q^4)] \cdot \upsilon_{QIS}/\upsilon_0 \tag{8}$$

Intriguingly, the factor $(k_q^0 - k_q^4)/(q - k_q^4)$ is equal to $-10/17$ for all spin values and methods (q); this is the basis for the 'unified' representation, wherein both MQMAS and STMAS spectra can be presented with the same axis system [25].

For the Q-shear transformation, the spectral window in *hertz* scales according to

$$SW_Q(Hz) = SW_1(Hz)/(1 + |q|) \tag{9}$$

The chemical shift is simply zero, whereas for the quadrupolar interaction both the isotropic and the anisotropic parts are present in F_Q (in *hertz*)

$$\begin{aligned} \upsilon_Q^{F_Q} &= [(k_q^0 - q)/(1 + |q|)] \cdot \upsilon_{QIS} + [(k_q^4 - q)/(1 + |q|)] \cdot \upsilon_4(\theta, \phi) \\ &= \kappa_Q^0 \cdot \upsilon_{QIS} + \kappa_Q^4 \cdot \upsilon_4(\theta, \phi) \end{aligned} \tag{10}$$

Considering that the chemical shift is absent along the F_Q axis, presenting the axis in *hertz* would be preferable, thereby minimizing the confusion of using *ppm* units and avoiding chemical shift scaling. Since the value of υ_{QIS} in F_Q is always positive after Q-shearing, it is sometimes advantageous to shift the zero frequency position from the center to the edge of the F_Q window. This way the spectral window is used optimally to cover the quadrupolar shift and avoid folding/aliasing (see Fig. 3c). In general, these shear transformations are a change in the combination of the three frequency parameters: the isotropic chemical shift υ_{CS}, quadrupolar-induced shift υ_{QIS}, and anisotropic quadrupolar shift $\upsilon_4(\theta, \phi)$,

$$\upsilon^{F_\Gamma} = \kappa_\Gamma^{CS} \cdot \upsilon_{CS} + \kappa_\Gamma^0 \cdot \upsilon_{QIS} + \kappa_\Gamma^4 \cdot \upsilon_4(\theta, \phi) \tag{11}$$

$$\upsilon^{F_2} = \upsilon_{CS} + \upsilon_{QIS} + \upsilon_4(\theta, \phi) \tag{12}$$

where Γ can be *iso* or Q for the isotropic- and Q-sheared representations. Note that the symbol κ is used to represent coefficients of the different interactions along the indirect dimension *after* shearing, as opposed to k which denote their counterparts *before* shearing. In the original representations, all three properties are present along the F_1 dimension with $\kappa_\Gamma^{CS} = q$, $\kappa_\Gamma^0 = k_q^0$ and $\kappa_\Gamma^4 = k_q^4$. Because there are two spectral dimensions available, only one of the properties can be completely isolated/removed by shearing (e.g., $\kappa_{iso}^4 = 0$ for isotropic shearing or $\kappa_Q^{CS} = 0$ for Q-shearing) while the other two remain convoluted. Isotropic shearing provides high-resolution spectra in F_{iso} and anisotropic broadening parallel to F_2, which seems most convenient for interpretation of crystalline compounds. However, for disordered samples a characteristic second-order line shape is often lacking and a combination of distributions from chemical and quadrupolar-induced shifts would remain in F_{iso}. Q-shearing removes chemical shift distribution from F_Q, thus allowing analysis of quadrupolar shift distributions for amorphous compounds, but gives broadened spectra in both dimensions for crystalline compounds. Therefore, being aware that neither shearing method provides perfect isolation of all parameters, users are left to decide which method is more appropriate for their samples. Table 2 lists the $(\kappa_\Gamma^{CS}, \kappa_\Gamma^0, \kappa_\Gamma^4)$ ratios and scaling factors for the shearing of different experiments and spin numbers.

4. Applications of *Q*-shearing

Fig. 1a shows a simulated 3QMAS spectrum for a spin-5/2 in its original representation which consists of three sites with ridges tilted at slope k_3^4. Due to the chemical shift difference between sites, separation of the peaks exceeds the F_1 spectral window restricted by t_1 synchronization. Indeed, given that chemical shift evolution is amplified by a factor equal to the coherence level (q) selected during t_1, it is not a rare occurrence for chemical shift spread to exceed the rotor-synchronized F_1 window, particularly at high magnetic fields. Peaks lying outside the window are either aliased or folded-in. In this instance, the peak centered at $F_2 \approx -4.4$ kHz is supposed to be at $F_1 \approx -12.3$ kHz, but instead appears at $F_1 \approx -2.3$ kHz due to aliasing. After isotropic shearing (by

Table 2
Ratios between the direct and indirect dimension chemical and quadrupolar shift frequencies (in *hertz*) and spectral width scaling factors for isotropic- and Q-shearing of STMAS and MQMAS experiments with spin S up to 9/2.

q	1Q STMAS 1		2Q STMAS 2		3QMAS 3		5QMAS 5		7QMAS 7		9QMAS 9	
Γ	*iso*	*Q*	*iso*	*Q*	*iso*	*Q*	*iso*	*Q*	*iso*	*Q*	*iso*	*Q*
$S = 3/2$	1[a] −10/17[b] 17/9[c]	−3/2[d] −17/18[e]	17/10 −1 17/9	−1 −17/27	17/8 −5/4 34/9	−3/2 −17/18	–	–	–	–	–	–
$S = 5/2$	17/31 −10/31 17/24	−9/16 −17/48	17/55 −2/11 17/24	−3/8 −17/72	17/31 −10/31 17/12	−9/16 −17/48	85/37 −50/37 85/12	−15/8 −85/72	–	–	–	–
$S = 7/2$	17/73 −10/73 17/45	−3/10 −17/90	17/118 −5/59 17/45	−1/5 −17/135	17/73 −10/73 34/45	−3/10 −17/90	17/10 −1 34/9	−1 −17/27	238/103 −140/103 476/45	−21/10 −119/90	–	–
$S = 9/2$	17/127 −10/127 17/72	−3/16 −17/144	17/199 −10/199 17/72	−1/8 −17/216	17/127 −10/127 17/36	−3/16 −17/144	85/131 −50/131 85/36	−5/8 −85/216	119/25 −14/5 119/18	−21/16 −119/144	85/37 −50/37 85/6	−9/4 −17/12

[a] Ratio between the F_{iso} and F_2 isotropic chemical shifts (in *hertz*) after isotropic shearing, $\kappa_{iso}^{CS} = (q - k_q^4)/(1 + |k_q^4|)$ (see Eq. (5)).
[b] Ratio between the F_{iso} and F_2 isotropic quadrupolar-induced shifts (in *hertz*) after isotropic shearing, $\kappa_{iso}^0 = (k_q^0 - k_q^4)/(1 + |k_q^4|)$ (see Eq. (6)).
[c] Scaling factor for conversion of F_1 from units of *hertz* to *ppm* after isotropic shearing, $SW_1(Hz)/[SW_{iso}(ppm) \cdot \upsilon_0] = (q - k_q^4)$ (see Eq. (7)).
[d] Ratio between the F_Q and F_2 quadrupolar-induced shifts (in *hertz*) after Q-shearing, $\kappa_Q^0 = (k_q^0 - q)/(1 + |q|)$ (see Eq. (10)).
[e] Ratio between the F_Q and F_2 anisotropic quadrupolar shifts (in *hertz*) after Q-shearing, $\kappa_Q^4 = (k_q^4 - q)/(1 + |q|)$ (see Eq. (10)). In all cases, the spectral window along F_1 (in *hertz*) is scaled according to Eqs. (4) and (9).

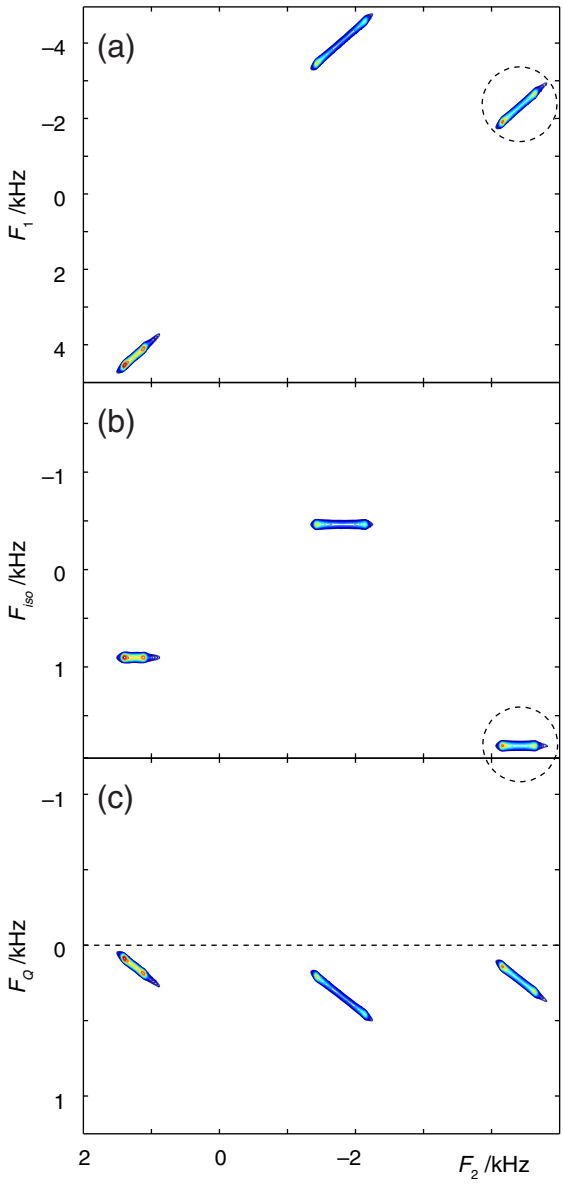

Fig. 1. Simulation of a z-filtered 3QMAS spectrum with rotor-synchronized t_1 for three spin-5/2 sites using the parameters: υ_0 = 156.6 MHz, 10 kHz MAS frequency, $\{\upsilon_{CS}$ [Hz], C_Q[MHz]} = {1500, 2.6}, {−1200, 4.0}, {−4000, 3.3} and $\eta_Q = 0$. Simulated 3QMAS spectrum shown in the (a) original, (b) isotropic and (c) Q-shear representations. Site circled with a dashed line in (a) and (b) appears at an incorrect position due to aliasing in F_1 and F_{iso}. The transmitter frequency is set at 0 kHz in both dimensions.

the factor $k_3^4 = 19/12$), which aligns anisotropic quadrupolar broadening parallel to F_2, the site at $F_2 \approx -4.4$ kHz remains aliased and appears at $F_{iso} \approx 1.8$ kHz instead of its correct position at $F_{iso} \approx -2.1$ kHz (Fig. 1b). The problem of aliasing would be more pronounced for experiments with negative k_q^4 values, such as 3QMAS of spin-3/2, since the chemical shift remains amplified by the factor $\kappa_{iso}^{CS} = (q - k_q^4)/(1 + |k_q^4|)$. Fig. 1c shows the spectrum processed using Q-shearing (by the factor $q = 3$), which aligns the chemical shift axis parallel to F_2, thus completely eliminating chemical shift spread in F_Q. The displacement along the F_Q axis of the center of gravity for each ridge is given by the quadrupolar-induced shift υ_{QIS}. Hence, aliasing in F_Q due to chemical shift is avoided as long as the anisotropic quadrupolar broadening fits within the indirect dimension spectral window. For applied MAS frequencies which separate the centerband from adjacent spinning sidebands, a rotor-synchronized F_1 (i.e., SW_1 = MAS frequency) will be sufficient to encompass the quadrupolar broadened peaks.

Fig. 2 shows a ^{45}Sc ($S = 7/2$) 3QMAS NMR spectrum of $0.65Pb(Sc_{2/3}W_{1/3})O_3$–$0.35PbTiO_3$ (PSW35PT) processed without shearing and with isotropic- and Q-shearing. The Sc^{3+}, Ti^{4+}, and W^{6+} ions occupy B-sites in the perovskite lattice of this material, and their positional and compositional disorder controls its relaxor ferroelectric properties [28]. This particular sample displays one broadened peak. In its original representation (Fig. 2a) the peak extends across F_1 due to the broadening and results in aliasing. Isotropic shearing (by the factor $k_3^4 = 101/45$) aligns quadrupolar patterns parallel to F_2, which serves to differentiate peaks from different sites in F_{iso}. However, for such disordered samples isotropic shearing tends to show peaks broadened by both chemical and quadrupolar shift distributions (Fig. 2b). In the Q-sheared spectrum (Fig. 2c), the chemical shift becomes zero along F_Q and this dimen-

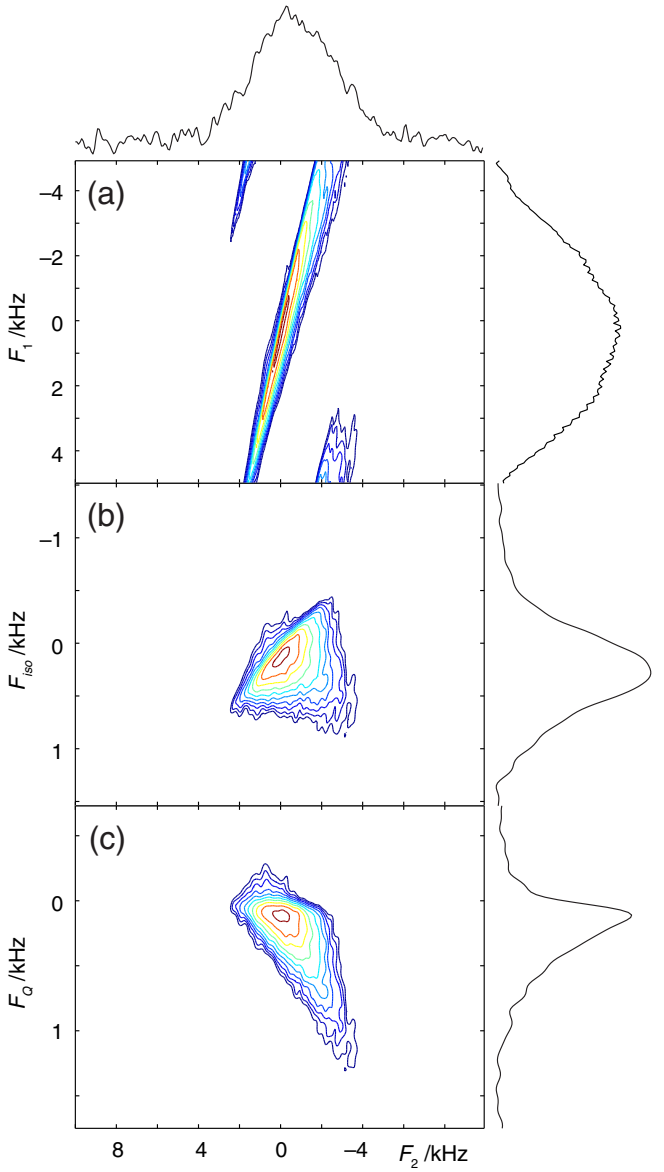

Fig. 2. ^{45}Sc ($S = 7/2$) 3QMAS spectrum of PSW35PT processed using (a) no shearing, (b) isotropic shearing and (c) Q-shearing. The spectrum in (c) was shifted in F_Q by a fifth of the spectral window to avoid any aliasing of peaks. The NMR spectrum was acquired at 14.1 T with MAS frequency of 10 kHz and a rotor-synchronized t_1. The transmitter frequency is set to 0 kHz in both dimensions. Base contours are set at 18% of the maximum intensity.

sion gives a direct visualization of only the quadrupolar shift. It should be reiterated that *all shear transformations are just a change of representation for the convenience of spectral interpretation.* The total information content remains *unchanged* from its original (3Q–1Q) representation.

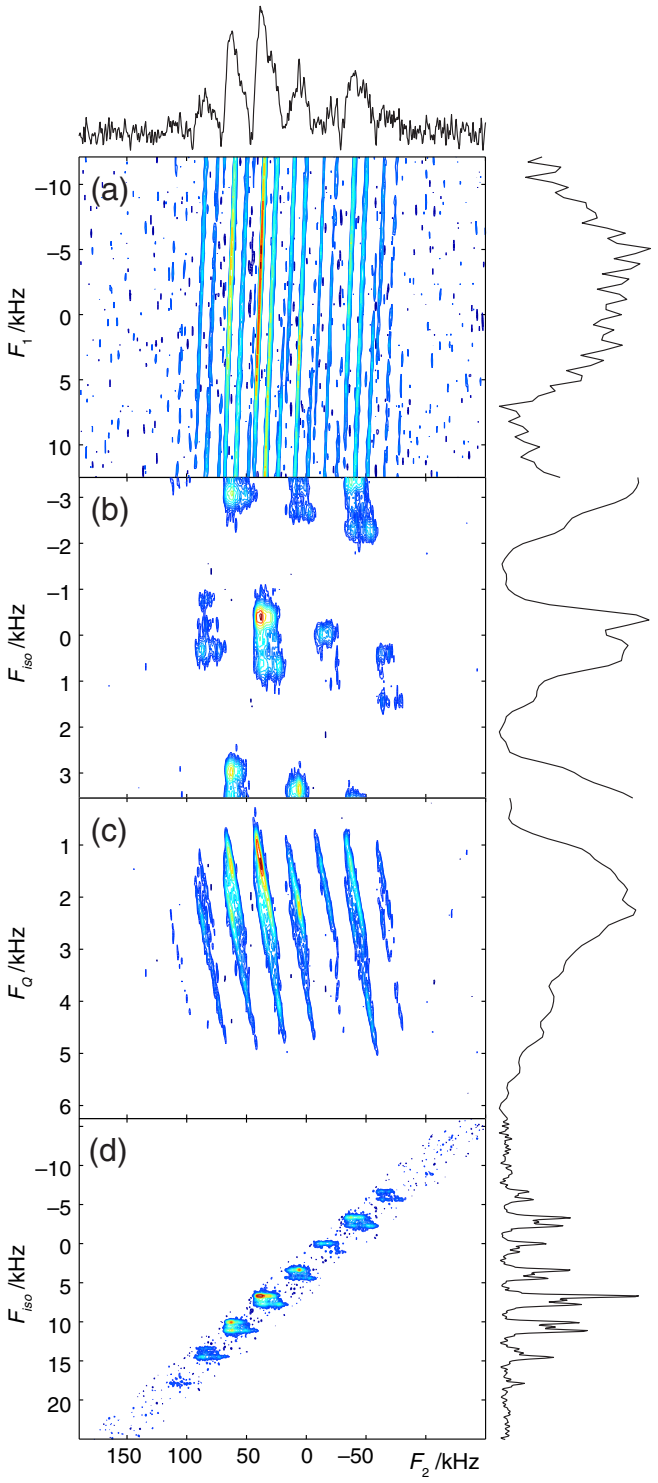

Fig. 3. ^{93}Nb ($S = 9/2$) 3QMAS spectrum of the dodecaniobate Keggin material $Na_{16}[SiNb_{12}O_{40}]\cdot 4H_2O$ processed using (a) no shearing, (b) isotropic shearing and (c) Q-shearing. (d) Spectrum in isotropic representation after Q-shearing and expansion of the F_{iso} spectral window by zero-filling in the frequency-domain. The spectrum in (c) was shifted in F_1 by half of the spectral window to avoid any aliasing of peaks. The NMR spectrum was acquired at 19.6 T with MAS frequency of 25 kHz and a rotor-synchronized t_1. The transmitter frequency is set to 0 kHz in both dimensions. Base contours are set at 8% of the maximum intensity in (a–c), and at 6% for (d) in order to highlight the original spectral area (the noise floor) in comparison to the final spectrum.

Fig. 3a shows a ^{93}Nb ($S = 9/2$) 3QMAS spectrum of the dodecaniobate Keggin material $Na_{16}[SiNb_{12}O_{40}]\cdot 4H_2O$ in its original representation. This sample has three crystalline sites with similar chemical shifts, large quadrupolar couplings and large shielding anisotropy. Even with a 25 kHz MAS frequency, numerous spinning sidebands appear and are barely resolved at 19.6 T. The shifted-echo 3QMAS spectrum was acquired with rotor-synchronized t_1 such that spinning sidebands are aliased in F_1, appearing only along the F_2 dimension. Due to the extent to which peaks and spinning sidebands are multiply aliased in F_1, the spectrum in the original representation appears completely undecipherable. The isotropically sheared spectrum in Fig. 3b shows three partially resolved sites. However, the spinning sidebands are no longer aligned only along F_2 because shearing is applied using a non-integer factor ($k_3^4 = 91/36$ in this case). The projection along the small F_{iso} window becomes broadened and crowded by the spinning sidebands. In contrast, Q-shearing is always performed by an integer number ($q = 3$ in this case), causing the centerband and sidebands to remain aligned along F_2, for which a large spectral window can easily be set to cover all spinning sidebands (Fig. 3c). In this instance, the ^{93}Nb spectrum was shifted upwards by half the F_Q spectrum width to avoid any peak aliasing after Q-shearing.

Q-shearing may also be used as an intermediate step to obtain an isotropically sheared spectrum free of aliasing. After Q-shearing, the spectrum is zero-filled in the frequency-domain along both directions of F_Q such that the original spectral region remains centered. The frequency-zero-filled spectrum can then be sheared back into its original representation before applying isotropic shearing. For Q-shearing, these two transformations can be carried in one step using the factor $\kappa_Q^4 = (k_q^4 - q)/(1 + |q|)$, i.e., $-17/144$ in this case (note the $1 + |q|$ factor from change of the spectral window in Eq. (9)). The F_{iso} scale remains the same as for the typical isotropic representation, except the spectral window is expanded by a factor corresponding to the ratio of data points before and after frequency-domain zero-filling. The resulting spectrum shows ordered spinning sidebands along both the F_{iso} and F_2 dimensions, without aliasing of spinning sidebands (Fig. 3d). The frequency-zero-filling cannot be applied directly to the original representation because the spread of individual sidebands already exceeds the F_1 spectral window restricted by the spinning frequency. In some cases, shearing by an integer factor other than q may also be used as the intermediate step to remove aliasing/folding along the indirect dimension. In that case the chemical shift is not completely removed, however, the spread due to the quadrupolar broadening may be less than when Q-shearing. Ultimately, as long as the shearing factor is an integer, the spinning sidebands will only be aliased such that they remain aligned along F_2, and the best choice of integer factor will depend on the spin quantum number and spread of the chemical shift and quadrupolar broadening. An interesting case is the shearing of 2Q STMAS spectra by a factor of 1, which converts 2Q STMAS spectra into the same exact representation as 1Q STMAS spectra.

5. Conclusions

Q-shearing provides efficient use of the spectral area and is particularly useful at high magnetic fields since typical isotropic shearing requires large spectral windows to cover the field-proportioned MQ chemical shift, while the Q-shear representation needs only a small spectral window sufficient to cover the quadrupolar-induced and anisotropic second-order shifts (which are reduced

by high fields). In addition, *Q*-shearing may be used to unscramble the folding/aliasing arising due to large spreads in chemical shift or the presence of numerous spinning sidebands by providing a representation which can be zero-filled in the frequency-domain to expand the F_{iso} spectrum width.

Acknowledgments

This work is supported by the National High Magnetic Field Laboratory through National Science Foundation Cooperative Agreement DMR0654118 and by the State of Florida. Todd M. Alam (Sandia National Laboratories) is thanked for providing the $Na_{16}[SiNb_{12}O_{40}]\cdot 4H_2O$ sample. Work by RLV and GLH was supported by NSF Grant CHE0079136 and the Office of Naval Research, Contract N000140310661. JT and JPA thank the Bruker company for funding.

References

[1] L. Frydman, J.S. Harwood, Isotropic spectra of half-integer quadrupolar spins from bidimensional magic-angle-spinning NMR, J. Am. Chem. Soc. 117 (1995) 5367–5368.
[2] Z.H. Gan, Isotropic NMR spectra of half-integer quadrupolar nuclei using satellite transitions and magic-angle spinning, J. Am. Chem. Soc. 122 (2000) 3242–3243.
[3] P.K. Madhu, A. Goldbourt, L. Frydman, S. Vega, Sensitivity enhancement of the MQMAS NMR experiment by fast amplitude modulation of the pulses, Chem. Phys. Lett. 307 (1999) 41–47.
[4] A.P.M. Kentgens, R. Verhagen, Advantages of double frequency sweeps in static, MAS and MQMAS NMR of spin $I = 3/2$ nuclei, Chem. Phys. Lett. 300 (1999) 435–443.
[5] G. Wu, D. Rovnyak, R.G. Griffin, Quantitative multiple-quantum magic-angle-spinning NMR spectroscopy of quadrupolar nuclei in solids, J. Am. Chem. Soc. 118 (1996) 9326–9332.
[6] A. Goldbourt, P.K. Madhu, Multiple-quantum magic-angle spinning: high-resolution solid state NMR Spectroscopy of half-integer quadrupolar nuclei, Monatshefte Fur Chemie 133 (2002) 1497–1534.
[7] Z.H. Gan, H.T. Kwak, Enhancing MQMAS sensitivity using signals from multiple coherence transfer pathways, J. Magn. Reson. 168 (2004) 346–351.
[8] J.P. Amoureux, L. Delevoye, S. Steuernagel, Z. Gan, S. Ganapathy, L. Montagne, Increasing the sensitivity of 2D high-resolution NMR methods applied to quadrupolar nuclei, J. Magn. Reson. 172 (2005) 268–278.
[9] N. Malicki, L. Mafra, A.A. Quoineaud, J. Rocha, F. Thibault-Starzyk, C. Fernandez, Multiplex MQMAS NMR of quadrupolar nuclei, Solid State Nucl. Magn. Reson. 28 (2005) 13–21.
[10] S.P. Brown, S. Wimperis, Two-dimensional multiple-quantum MAS NMR of quadrupolar nuclei: a comparison of methods, J. Magn. Reson. 128 (1997) 42–61.
[11] J.P. Amoureux, C. Fernandez, S. Steuernagel, Z filtering in MQMAS NMR, J. Magn. Reson. Ser. A 123 (1996) 116–118.
[12] Z.H. Gan, Satellite transition magic-angle spinning nuclear magnetic resonance spectroscopy of half-integer quadrupolar nuclei, J. Chem. Phys. 114 (2001) 10845–10853.
[13] D. Massiot, Sensitivity and lineshape improvements of MQ-MAS by rotor-synchronized data acquisition, J. Magn. Reson. Ser. A 122 (1996) 240–244.
[14] Z. Gan, P.L. Gor'kov, T.A. Cross, A. Samoson, C. Huguenard, F. Taulelle, D. Massiot, A.A. Mrse, L.G. Butler, G. Hoatson, High-field, fast-speed and satellite transition MAS NMR of quadrupolar nuclei, 43rd Rocky Mountain Conference on Analytical Chemistry, 2001.
[15] H.T. Kwak, Z.H. Gan, Double-quantum filtered STMAS, J. Magn. Reson. 164 (2003) 369–372.
[16] J.T. Ash, N.M. Trease, P.J. Grandinetti, Separating chemical shift and quadrupolar anisotropies via multiple-quantum NMR Spectroscopy, J. Am. Chem. Soc. 130 (2008) 10858.
[17] I. Hung, A. Wong, A.P. Howes, T. Anupold, A. Samoson, M.E. Smith, D. Holland, S.P. Brown, R. Dupree, Separation of isotropic chemical and second-order quadrupolar shifts by multiple-quantum double rotation NMR, J. Magn. Reson. 197 (2009) 229–236.
[18] A. Medek, J.S. Harwood, L. Frydman, Multiple-quantum magic-angle spinning NMR: A new method for the study of quadrupolar nuclei in solids, J. Am. Chem. Soc. 117 (1995) 12779–12787.
[19] J.P. Amoureux, High-resolution solid-state NMR for spin 3/2 and 9/2 – the Multiquantum Transitions Method, Solid State Nucl. Magn. Reson. 2 (1993) 83–88.
[20] P.J. Grandinetti, Y.K. Lee, J.H. Baltisberger, B.Q. Sun, A. Pines, Side-band patterns in dynamic-angle-spinning NMR, J. Magn. Reson. Ser. A 102 (1993) 195–204.
[21] K.J. Pike, S.E. Ashbrook, S. Wimperis, Two-dimensional satellite-transition MAS NMR of quadrupolar nuclei: shifted echoes, high-spin nuclei and resolution, Chem. Phys. Lett. 345 (2001) 400–408.
[22] S.P. Brown, S.J. Heyes, S. Wimperis, Two-dimensional MAS multiple-quantum NMR of quadrupolar nuclei, removal of inhomogeneous second-order broadening, J. Magn. Reson. Ser. A 119 (1996) 280–284.
[23] R.R. Ernst, G. Bodenhausen, A. Wokaun, Principles of Nuclear Magnetic Resonance in One and Two Dimensions, Oxford University Press, New York, 1987.
[24] D. Massiot, F. Fayon, M. Capron, I. King, S. Le Calve, B. Alonso, J.O. Durand, B. Bujoli, Z.H. Gan, G. Hoatson, Modelling one- and two-dimensional solid-state NMR spectra, Magn. Reson. Chem. 40 (2002) 70–76.
[25] J.P. Amoureux, C. Huguenard, F. Engelke, F. Taulelle, Unified representation of MQMAS and STMAS NMR of half-integer quadrupolar nuclei, Chem. Phys. Lett. 356 (2002) 497–504.
[26] S.E. Ashbrook, S. Wimperis, High-resolution NMR of quadrupolar nuclei in solids: the satellite-transition magic angle spinning (STMAS) experiment, Prog. Nucl. Magn. Reson. Spectrosc. 45 (2004) 53–108.
[27] P.P. Man, Scaling and labeling the high-resolution isotropic axis of two-dimensional multiple-quantum magic-angle-spinning spectra of half-integer quadrupole spins, Phys. Rev. B 58 (1998) 2764–2782.
[28] P. Juhas, P.K. Davies, M.A. Akbas, Chemical order and dielectric properties of lead scandium tungstate relaxors, AIP Conf. Proc. 626 (2002) 108–116.